AD-A116 801 GEORGIA INST FOR RESEARCH ATHENS F/G 13/11
INTERACTION OF OSCILLATIONS OF CHANNEL FLOW AND FLOW SEPARATION--ETC(U)
AUG 81 E W PRICE, J E HUBBARTT, W C STRAHLE N60530-79-M-0W93
NWC-TP-6302
UNCLASSIFIED NL

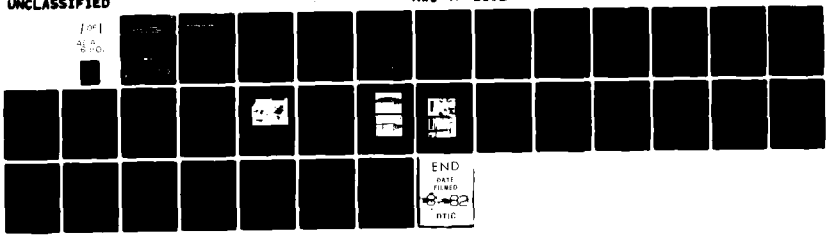

END
DATE FILMED
8-82
DTIC

AD A116801

NWC TP 6302

(12)

Interaction of Oscillations of Channel Flow and Flow Separation at Duct Discontinuities

by
E. W. Price, J. E. Hubbartt, W. C. Strahle,
E. A. Oguz and P. M. Sagdeo
Georgia Institute of Technology
for the
Research Department
Naval Weapons Center

AUGUST 1981

NAVAL WEAPONS CENTER
CHINA LAKE, CALIFORNIA 93555

Approved for public release; distribution unlimited.

DTIC
ELECTE
JUL 9 1982
S D
B

82 07 09 017

DTIC FILE COPY

Naval Weapons Center

AN ACTIVITY OF THE NAVAL MATERIAL COMMAND

FOREWORD

This facsimile report, based on an original manuscript submitted by the authors, represents the final report for work performed under Naval Weapons Center (NAVWPNCEN) Contract Number N60530-79-M-DW93. Professor E. W. Price, Georgia Institute of Technology, Atlanta, Georgia, was principal investigator and Mr. H. B. Mathes of NAVWPNCEN was technical coordinator. The report covers work performed between September 1979 and August 1980 on NASA Defense Purchase Request Number H-14156.B.

The results of this work were presented at the 17th JANNAF Combustion Meeting in September 1980 at the NASA Langley Research Center, Hampton, Virginia, and published in the proceedings of that meeting (CPIA Publication Number 329).

Due to a high level of interest in the subject, the information is released as a NAVWPNCEN Technical Publication so that it will be readily available to motor stability specialists.

This report is released at the working level for information and does not represent the final judgement of the Naval Weapons Center.

Approved by
E. B. ROYCE, *Head*
Research Department
4 August 1981

Under authority of
J. J. LAHR
Capt. U.S. Navy
Commander

Released for publication by
R. M. HILLYER
Technical Director

NWC Technical Publication 6302

Published by . . . . . Research Department
Collation . . . . . Cover, 16 leaves
First printing . . . . . 155 unnumbered copies

UNCLASSIFIED

SECURITY CLASSIFICATION OF THIS PAGE *(When Data Entered)*

REPORT DOCUMENTATION PAGE	READ INSTRUCTIONS BEFORE COMPLETING FORM
1. REPORT NUMBER: NWC TP 6302	2. GOVT ACCESSION NO.: AD-A116 801
	3. RECIPIENT'S CATALOG NUMBER:
4. TITLE (and Subtitle): INTERACTION OF OSCILLATIONS OF CHANNEL FLOW AND FLOW SEPARATION AT DUCT DISCONTINUITIES	5. TYPE OF REPORT & PERIOD COVERED: FACSIMILE – FINAL SEPT 1979 – AUG 1980
	6. PERFORMING ORG. REPORT NUMBER:
7. AUTHOR(s): E. W. PRICE, J. E. HUBBARTT, W. C. STRAHLE, E. A. OGUZ, and P. M. SAGDEO	8. CONTRACT OR GRANT NUMBER(s): N60530–79–M–DW93
9. PERFORMING ORGANIZATION NAME AND ADDRESS: GEORGIA INSTITUTE OF TECHNOLOGY ATLANTA, GEORGIA	10. PROGRAM ELEMENT, PROJECT, TASK AREA & WORK UNIT NUMBERS: H–14156.B
11. CONTROLLING OFFICE NAME AND ADDRESS: NAVAL WEAPONS CENTER CHINA LAKE, CALIFORNIA	12. REPORT DATE: AUGUST 1981
	13. NUMBER OF PAGES: 28
14. MONITORING AGENCY NAME & ADDRESS(if different from Controlling Office)	15. SECURITY CLASS. (of this report): UNCLASSIFIED
	15a. DECLASSIFICATION/DOWNGRADING SCHEDULE

16. DISTRIBUTION STATEMENT *(of this Report)*

APPROVED FOR PUBLIC RELEASE; DISTRIBUTION UNLIMITED

17. DISTRIBUTION STATEMENT *(of the abstract entered in Block 20, if different from Report)*

18. SUPPLEMENTARY NOTES

19. KEY WORDS *(Continue on reverse side if necessary and identify by block number)*

VORTEX FLOW
MEAN VELOCITY
FREESTREAM

20. ABSTRACT *(Continue on reverse side if necessary and identify by block number)*

(SEE BACK OF FORM)

DD FORM 1 JAN 73 1473 EDITION OF 1 NOV 65 IS OBSOLETE
S/N 0102-014-6601 |

UNCLASSIFIED

SECURITY CLASSIFICATION OF THIS PAGE *(When Data Entered)*

(U) *Interaction of Oscillations of Channel Flow and Flow Separation at Duct Discontinuities*, by E. W. Price, J. E. Hubbartt, W. C. Strahle, E. A. Oguz, and P. M. Sagdeo. Georgia Institute Of Technology, Atlanta, Georgia. China Lake, Calif., Naval Weapons Center, August 1981, 27 pp. (NWC TP 6302, publication UNCLASSIFIED.)

(U) The subject of vortex flow and coupling between vortices and acoustic wave motions in rocket motor chambers has become a topic of high interest to rocket motor stability specialists in the past several years. Although the phenomenon was first noted to be a significant factor in the stability of very large booster motors, recent experiences in tactical-sized motors indicate that vortex-acoustic wave interactions can become an important factor in determining acoustic wave amplitudes in all solid-propellant rocket motors, regardless of size.

(U) A two-dimensional experiment was used to study the flow fluctuations in the separated region resulting from a wall-slot-step (convergent step). This geometry corresponds to the geometry present in a segmented solid rocket motor in the region of the ends of adjoining segments. A modulated tunnel flow of controlled oscillation frequency was used, and the effect on flow fluctuations in the separated region was examined by hot-wire velocity measurements. The transfer function between free stream oscillations and separated flow fluctuations at the driven frequency was determined over a range of frequencies and main stream flow velocities. The transfer function exhibited a frequency dependence with maximum in the 10-25 Hz range, with the maximum occurring at higher frequency when the mean flow velocity was higher.

CONTENTS

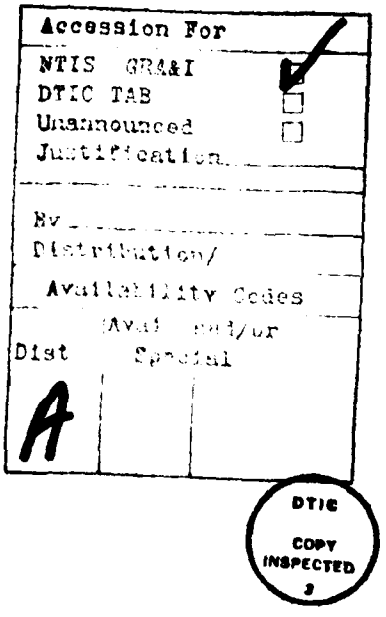

DTIC
COPY
INSPECTED

INTERACTION OF OSCILLATIONS OF CHANNEL FLOW AND FLOW SEPARATION AT DUCT DISCONTINUITIES

E. W. Price, J. E. Hubbartt, W. C. Strahle, E. A. Oguz and P. M. Sagdeo
Georgia Institute of Technology
Atlanta, Georgia

ABSTRACT

A two-dimensional experiment was used to study the flow fluctuations in the separated region resulting from a wall-slot-step (convergent step). This geometry corresponds to the geometry present in a segmented solid rocket motor in the region of the ends of adjoining segments. A modulated tunnel flow of controlled oscillation frequency was used, and the effect on flow fluctuations in the separated region was examined by hot-wire velocity measurements. The transfer function between free stream oscillations and separated flow fluctuations at the driven frequency was determined over a range of frequencies and main stream flow velocities. The transfer function exhibited a frequency dependence with maximum in the 10 - 25 Hz range, with the maximum occurring at higher frequency when the mean flow velocity was higher.

INTRODUCTION

Data from static firings of the NASA solid propellant shuttle booster motor has shown the presence of a low level pressure and thrust oscillation at a frequency suggestive of first longitudinal mode of the combustor cavity. Calculations of the cavity stability based on conventional combustion instability methods indicated that combustion excitation of any acoustic mode was improbable. However it has long been recognized that substantial "noise" is produced in the gas flow in a rocket motor, and that a measure of coupling between noise sources, mean flow, and cavity mode oscillations can lead to oscillations. In the case of the Shuttle SRM, the internal flow is affected by the fact that the propellant charge (and hence gas flow channel) has abrupt transitions due to the segmented design of the motor (Fig. 1), and it has been suspected that flow in the vicinity of the channel discontinuities might couple with axial mode oscillations. Such behavior has been observed in the past in duct flows with various wall discontinuities, but none simulated the situation in the segmented motor configurations. Knowledge of the details of the flow responsible for coupled behavior is not sufficient to permit avoidance by proper design--at least not within the constraints normally present in rocket motor design.

The objective of the present study was to determine whether a coupling did indeed occur between longitudinal oscillations and the "noise" sources normally present in the flow in the vicinity of the segment ends. In the process, it was hoped that some details of the flow behavior would also be revealed. Being a very limited investigation, it was proposed that the

---

* This work was supported by NASA via the U. S. Naval Weapons Center (Purchase Order No. N60530-79-M-DW93).

Approved for public release; distribution unlimited.

study be made in an available small wind tunnel, using a flat channel rather than a cylindrical one. The test model was simply a solid wall with a slot and a ledge, simulating the gap between propellant charge segments and simulating the inside diameter transition between adjoining ends of charge segments. The test facility was already equipped for flow visualization by smoke streamers, and hot-wire anemometers, and pitot-static tubes were available. Flow in the tunnel was induced by a blower on the exhaust side, and flow oscillations were produced by adding a rotating baffle in the exhaust duct. The question of presence or absence of coupling was addressed by Fourier analysis of concurrent records of velocity fluctuations observed in the freestream and in the separated flow region downstream of the "segment".

EXPERIMENTAL APPARATUS

AIR FLOW SYSTEM

The available wind tunnel is shown diagramatically in Fig. 2 in profile. The test section is 6.4 cm wide, with glass walls. The entrance section provides aerodynamically designed transitions to all four walls, with multiple screens at the inlet to minimize initial turbulence. Flow is induced by suction on the plenum chamber by a blower on the back of the unit. Flow velocity in the tunnel is varied by opening a by-pass door to the plenum. Prior to modifications for this study, the range of available tunnel velocities was 3-15 m/sec (values with the standard model in place).

Modification of the air flow system for oscillatory flow consisted primarily of introducing a motor-driven rotating baffle in the exhaust duct downstream of the blower. Preliminary calculations indicated that the natural filling-exhausting time of the system was short compared to the period of oscillation of interest in tests (5-20 Hz). However several baffle sizes were prepared because of uncertainty of oscillation levels needed for satisfactory measurement of velocity oscillations. As one would expect of a bulk mode oscillation, the amplitude of oscillations decreased with increasing frequency. Fig. 3 shows the arrangement of the exhaust duct for modulated flow. Measures were also taken to stiffen walls and windows in the tunnel to minimize pressure-induced vibrations that appeared to be compromising the measurements. However the data anomalies were later traced to other causes, and it remains uncertain how rigid duct walls need to be.

TEST MODELS

The details of the segmented motor geometry of concern in this study are shown in Fig. 4. In the motor, the downstream end of the propellant charge segment (A), is thinner than the end of the next segment, (B), so the wall flow must deflect into the freestream. In addition, the end surface of the upstream segment (A) is burning, so there is flow out of the slot into the mainstream. The face (B) of the downstream segment is partially inhibited by a plastic ring, which does not burn away as fast as the propellant, and protrudes into the channel after a period of operation (oscillations observed in motor firings occur in the later half of burning).

Considering the foregoing features of the Shuttle SRM configuration, the test duct was equipped with a model shown in Fig. 5. The model was assembled from lucite, and the flow ducts can be distinguished in the figure by the smoke trails. Flow from the slot was supplied by extension of the lower duct into the tunnel inlet. The model was made in two segments so that the spacing (slot width) could be adjusted. A second upstream segment was made that was the same height as the downstream one, thus permitting uniform wall tests (no slot). Plates were provided for the face of the downstream segment with different protrusion heights, to simulate inhibitor protrusion.

INSTRUMENTATION

Flow visualization in the unmodified wind tunnel was provided (as in Fig. 5), by an array of injectors mounted in the inlet and supplied with an oil-fog type of "smoke". This injector array was removed for most work, and smoke was supplied only to selected openings in the walls of the model.

A conventional pitot-static probe was used to determine mean flow velocities. This system uses variable capacitance Barocel pressure transducers with analog electrical output and digital read-out (CGS Scientific Datametrics Div., Type 501). The probe was used primarily to calibrate the hot-wire system.

The hot-wire anemometers consisted of three Flow Corporation Model 900-1 units with locally fabricated, fixed wire installations made of KOVAR wires 5 mm long. In most tests three wire outputs were recorded. Locations of wires are noted in Fig. 6. Most of the reported data are from Positions A and B.

Frequency of oscillation was measured for adjustment during tests by observing the rotating baffle with a strobe light. This method was not very accurate, and frequencies used in plotting data are based instead on outputs of the analysis of test records.

Data acquisition systems included a Hewlett-Packard Model 7004A X-Y plotter and a Hewlett-Packard Model 3968 A tape recorder, using a recording speed of 1 7/8 IPS (inches/sec). Fig. 7 shows a typical pen recording of the velocity fluctuations. Data reduction was accomplished on a Hewlett-Packard Model 5451 A Fourier analyzer, which provided power spectra, transfer function and coherence (primarily between A and B). Examples are shown in Fig. 8. Both sample figures illustrate behavior during oscillatory flow as measured at locations A and B. The peak in the power spectrum reflects the driven frequency during the test (the ordinate scale is logarithmic).

SYSTEM CHARACTERISTICS AND CALIBRATION

Ideally one would like to do an exact simulation of rocket motor conditions to assure relevant results, i.e., exact simulation of dimensions, gas transport properties, flow velocities, etc. Short of that, a theoretical study of relevant similarity parameters would be desirable as an aide to design of more convenient experiments. In the present limited

effort, neither of these options was feasible. Frequencies were selected to cover the relevant range in the Shuttle SRM. Mean flow velocities were lower, but of the same order as present in the rocket motor in the latter part of burning (and were set by capability of the available system). The gas was air at atmospheric pressure and temperature. Likewise the available apparatus determined the use of a two-dimensional model, which was also desired for compatability with optical flow visualization.

The range of freestream velocities normally available in the smoke tunnel is 3 m/s to 15 m/s. In most of the tests in the present study this range was reduced to the range of 2 m/s to 10 m/s because of blockage of the exhaust duct by the rotating baffle.

The range of frequencies used was from 4 to 24 Hz. Lower frequency was not considered relevant, and even 4 Hz was used only at the lowest mean flow velocity. Upper frequency was chosen in part by the fact that amplitude decreased with increasing frequency. Ultimately the choice of upper frequency was based on the trend of test results, which indicated a maximum in the transfer function: tests were run to high enough frequency to establish this trend.

Choice of amplitude of oscillations to be used is not a straightforward question. Fig. 9 shows the effect of the size of the rotating baffle on mean flow velocity when the baffle is held in the blocking position (without model in tunnel: ~ 20% higher with model). This result pertains to the maximum velocity (closed) position of the by-pass door (See Fig. 2). A baffle size of 70 cm^2 (22% maximum blockage) was used in most tests. Fig. 10 shows the drop-off in amplitude with closing frequency of the rotating baffle. The choice of amplitude relates to the manner of analysis and interpretation of results, and is discussed more fully later. Obviously it is necessary to use an amplitude large enough to be distinguishable above the flow noise at the location of the hot wires, but it was not possible to determine the minimum usable amplitude in advance of tests.

The most severe calibration problems related to the velocity measurements. In particular, two aspects of the problem merit note. First, the systems were calibrated by the pitot-static probe, but this could not be done for wires mounted near the channel walls because the pitot-static probe was too large to make valid measurements in the non-uniform flow near the wall and the wires were on fixed mountings at those locations. This problem was circumvented by calibrating the freestream hot wire (which was on a movable probe). This probe was used to calibrate the wall probe.

The second problem with the hot-wire calibration is the nonlinear response characteristic (Fig. 11). Thus the measurements of velocity oscillation amplitude also depend upon knowledge of the mean velocity. While the absolute values of velocity amplitudes were not used in interpretation of results, trends with frequency and freestream velocity were used. Accordingly, the mean velocity for each test (each hot wire) was determined during each Fourier analysis (using also the hot-wire calibration curves, Fig. 11), and the corresponding hot-wire response to velocity fluctuations was used in evaluating the actual velocity

fluctuations. This proved to be a minor correction for trends of results with frequency, as the mean velocity was not very sensitive to the driven frequency of the test. However the change in hot-wire sensitivity between the high and low ends of the mean velocity range tested was appreciable, and consideration of the effect was important in valid comparisons of test results at different mean flow velocities as described later.

RESULTS

GENERAL DESCRIPTION OF GAS FLOW

The nature of the flow in the vicinity of the wall gap (segment ends) is indicated in Fig. 5. The boundary layer separates upstream of the slot and deflects up over the flow injected from the slot. The slot flow moves outward while turning downstream, overshooting and returning towards the wall further downstream. The separated region beneath the slot flow shows strong and complicated vortex behavior. The flow is reattached about 8 step heights downstream of the slot.

The nature of spontaneous velocity oscillations is shown in Fig. 12, where Part a shows recorded fluctuations and Part b shows the power spectrum for location B. Fig. 7 and 8 showed similar results for a test with driven oscillations. The results show the freestream to be relatively free of fluctuations when oscillations are not introduced, and to exhibit sinusoidal oscillations when driven. The Position B wire indicated broad band noise when oscillations were not introduced, and a similar spectrum when driven, but with a large peak at the driven frequency (in all spectra, the abrupt drop-off at high and low frequencies are artifacts of the analyzer operational settings, i.e., these frequencies were not judged to be relevant to the present investigation). Inspection of fluctuation records such as Fig. 7 from many test conditions shows that the driven frequency was generally recognizable in the Position B record, but not dominant.*

Under conditions similar to Fig. 12 but with a smooth wall configuration, the record at the Position B hot-wire showed an oscillation similar to the free stream, with minimal flow noise, a result that was duplicated over a range of frequencies and flow velocities. (In the smooth wall configurations, Position B hot-wire was probably outside most of the boundary layer.)

DISCUSSION

The objective of the present study was to determine whether or not the flow fluctuations normally present in the separated flow region near a slot-step are responsive to streamwise oscillations in the mainstream flow. In the present experiment, the mainstream oscillations were independently driven, and were present in varying degree everywhere in the flow. The magnitude and frequency of the driven oscillations were measured

* The low frequency component of the fluctuations around 4 Hz was not actually periodic, did not show up in the Fourier analysis, and was apparently due to an irregular fluctuation in speed of the blower in the tunnel.

by the hot-wire probe in the mainstream, which was relatively free of other flow fluctuations. Similar measurements in the separated flow region showed the driven oscillations, and the wall-induced fluctuations. From Fig. 8a it is evident that the broad band self-noise of the separated flow is substantial, and that the power in the driven frequency is also large. There is no simple way to show how much of the fluctuation at the driven frequency is in direct response to the driving process, and how much is due to response of the separated flow to imposed oscillations. However, it was reasoned that the relative level of oscillations in the mainstream and separated region should be insensitive to the frequency of the driven oscillations if the oscillations were uncoupled with the separated flow source of the broad band noise. In that case a transfer function at the driven frequency would be independent of frequency.

The driven frequency transfer function was determined over a range of frequencies and mean velocities. The results are shown in Fig. 13. Each data point corresponds to the peak in the transfer function at the driven frequency (Fig. 8) of a particular test. The three lower curves correspond to series of tests at three different mean flow velocities. The upper curve is for the model with a projecting lip corresponding to the projection of an inhibitor on the segment end in the late-burning geometry of the motor. The transfer functions exhibit a pronounced frequency dependence, which is interpreted as a property of the coupling process between driven mainstream oscillations and the broad-band noise-generating processes in the slot-step flow. This interpretation is supported by the apparently systematic shift of the transfer function curves to higher frequency when the time constants in the flow are reduced by going to higher mean flow velocity. Of practical interest to the rocket motor problem is the large effect of the protruding inhibitor lip on the magnitudes of the transfer functions.

The present work was largely exploratory, using existing facilities with only moderate adaptation. The intent was to determine whether detailed measurements in the slot-step region could reveal anything about responsiveness of flow processes in that region to mainstream oscillations, and whether trends could be determined that would be helpful in dealing with the rocket motor problem. A wider and more systematic set of measurements would be required to deal completely with the range of situations in a segmented rocket motor. Further, consideration would have to be given in the motor problem to the complete duct flow, involving as it does a cylindrical channel with mass addition at the walls, a mean flow field with several slot-steps in series, and axial dependence of mean and perturbation flow velocity. The present results suggest that some benefit would be realized from direct study of the details of flow in the slot-step region, where minor changes in design would have major effects on the coupling between acoustic oscillations and the "slot-step" noise source.

APPENDIX A

DATA ANALYSIS PROCEDURES

The Fourier analysis equipment used in data reduction is capable of powerful operations in what is called "time series analysis". The signals analyzed contained both random and periodic signals, from the turbulence and imposed oscillation, and the equipment is capable of decomposing the entire signal into its frequency components. Of primary interest here is the information at the imposed frequency of oscillation. In general, the information at this frequency contains a combination of the periodic signal and a contaminant--the turbulence.

Let y_ω be the amplitude of the overall signal at frequency ω. Then

$$y_\omega = y_{\omega_p} + y_{\omega_t} \tag{1}$$

where y_{ω_p} is the periodic part of y_ω and y_{ω_t} is the contaminant, which may be turbulence, electronic noise, etc. For two signals, y_{ω_1} and y_{ω_2}, there exist several interesting relations, computed by the analysis equipment, which have been used in the data interpretation. These are the cross spectral density, the transfer function and the coherence function. For any sample record length, y_{ω_p} has a fixed phase reference whereas the phase of y_{ω_t} will vary from sample to sample, because the noise is a random function of time. Consequently, ensemble averaging can be used to advantage to separate the periodic and random parts of the signal. Denoting the ensemble averaging procedure by an overbar, the cross spectral density is constructed by

$$S_{12} = \overline{y^*_{\omega_1} y_{\omega_2}} = \overline{y^*_{\omega_{1_p}} y_{\omega_{2_p}}} \tag{2}$$

where an asterisk denotes a complex conjugate. Here, only the periodic part survives by the averaging procedure. The transfer function between signals 1 and 2 is defined by

$$H_{12} = \frac{S_{12}}{S_{11}} = \frac{\overline{y^*_{\omega_{1_p}} \, y_{\omega_{2_p}}}}{\overline{y^*_{\omega_{1_p}} \, y_{\omega_{1_p}}} + \overline{y^*_{\omega_{1_t}} \, y_{\omega_{1_t}}}} \tag{3}$$

$$= \frac{S_{12}}{S_{11_p} + S_{11_t}}$$

Here S_{11} is the autospectrum of signal 1 and contains two parts--the autospectrum of the periodic part and the contaminant. If the contaminant were zero then

$$H_{12_{clean}} = \frac{y_{\omega_{p_2}}}{y_{\omega_{p_1}}}$$

which is nothing more than the ratio of the two signals at the driven frequency. H_{12} contains both the amplitude ratio and phase difference. In the experiments here, the frequencies were so low that phase difference was negligible and the quantity of interest is $|H_{12}|$ which is merely the amplitude ratio of the two signals.

If the signals were both clean ($y_{\omega_t} = 0$) and the system were linear ($y_{\omega_{p_1}} \alpha \, y_{\omega_{p_2}}$), $|H_{12}|$ should be amplitude independent. This linearity was checked in the experiment. The cleanliness of the signal was checked by the coherence function, defined by

$$\gamma^2 = \frac{|S_{12}|^2}{S_{11}\, S_{12}}$$

It is readily checked that $\gamma^2 = 1$ when $S_{11_t} = S_{22_t} = 0$; that is, when free of contaminants, $\gamma^2 = 1$. Moreover, when contaminants dominate, $\gamma^2 = 0$. Since, from Eq. (3), H_{12} cannot be determined independently of the contaminant, if the contaminant is large, only runs where γ^2 is close to unity are accepted.

Summarizing, only results at the driven frequency were desired. The coherence function was used to insure data quality and the end item of interest was the amplitude ratio of the two signals at the driven frequency. System linearity was checked by analyzing the trend of the amplitude ratio with signal amplitude. For a periodically driven system with small contamination there will always exist $|H_{12}|$.

APPENDIX B

COHERENCE

The velocity fluctuations at two different locations in the flow system will look alike if the primary cause of fluctuation is the periodic driven oscillation. The coherence function is a measure of the relationship between the periodic content at two different points in the flow. The coherence between velocity fluctuations at Positions A and B would have a value of one at the driven frequency if no other fluctuations having driven frequency content were present at the hot-wire sites. In the present flow system, the flow in the separated region contains a broad spectrum of fluctuations that are locally generated and not manifested at the freestream hot-wire location (Fig. 7 and 12). Under these conditions, the coherence at the driven frequency must be less than one, the actual value depending upon the intensity of the driven frequency component of the locally generated fluctuations compared to the driven oscillations at that point (B). A high coherence at the driven frequency may occur because

a) the noise level (locally generated driven frequency component at B) is low
b) the driving amplitude is so large it overwhelms the noise level
c) the second (B position) hot wire is so located in the flow that driven oscillations are large compared to noise (e.g., when a smooth wall is used)
d) the driven oscillations couple strongly with the noise generation to give more fluctuation at driven frequency, and less over the rest of the frequency domain.

Situations a - c are all mathematically equivalent, but occurred in the present work for independent experimental reasons.

In general, the Fourier analyses showed very low coherence except at the driven frequency (see example in Fig. 8), and coherence above 0.7 at the driven frequency (when the "standard baffle", see Fig. 3, 9, was used to oscillate the flow). The transfer function at driven frequency is shown as a function of driven frequency in Fig. 14. When a smooth (flat) duct wall was used the coherence values were nearly one (see dot-dash line in Fig. 14), reflecting the low level of local flow noise and the increased penetration of the driven oscillations to the B-Position hot-wire in the absence of flow separation. In the slot-step configuration, lower values of coherence at driven frequency resulted, still generally above 0.7. When the coherence is much less than this, the values of the transfer function (usually lower than the trend) were considered to be of doubtful validity.

The points in Fig. 14 that show low coherence merit some notice in the context of design of future experiments. These points reflect four trends that are related to different test conditions.

a) At 19 Hz there are three points with distinctive symbols (solid star, diamond and square) that resulted from standard test conditions with 9.2 m/s mean flow velocity setting, but different driven amplitudes (different baffle sizes). The lower coherence corresponds to decreased driven amplitude relative to local noise as baffle size is reduced. This effect was probably further enhanced by a modest increase in mean flow velocity and in separated flow noise that occurs when baffle size is reduced. In such tests, the driven oscillation is at its minimum value relative to the local flow noise.

b) In a frequency range around 13 Hz, there was a tendency for driven frequency transfer functions to be erratic and below the overall trend (Fig. 13). In such tests, the coherence was also low (Fig. 14). The reason for this anomaly was not determined. The transfer function values for such tests were considered to be irrelevant to the test objectives as only coherent behavior is relevant to the problem of flow excitation of freestream oscillations.

c) There is apparently a systematic trend of decreasing coherence with decreasing mean flow velocity. This trend cannot be interpreted usefully, because it reflects an interplay of competing effects. High mean flow rate causes high noise level (low coherence). But the freestream oscillation amplitude is also higher in this system at high mean flow rate, which affects coherence in the opposite direction (high coherence). The scope of the effort did not permit separation of these effects, leaving the meaning of the trend of coherence with mean flow velocity uncertain. This is not considered to be a serious outcome, as the primary interpretation of results follows from the transfer function, and coherence is used mainly to validate the data points.

d) There is a trend to decreasing coherence with increasing frequency (particularly at low mean flow velocity). This trend reflects the decreasing amplitude of driven oscillations (see Fig. 10) with increasing frequency. However, this trend is apparently countered by the coupled response of flow noise to the driven oscillations (reflected by the increasing transfer function, described in Fig. 13), which keeps the coherence up in spite of declining driven amplitude until the coupled response starts to drop off.

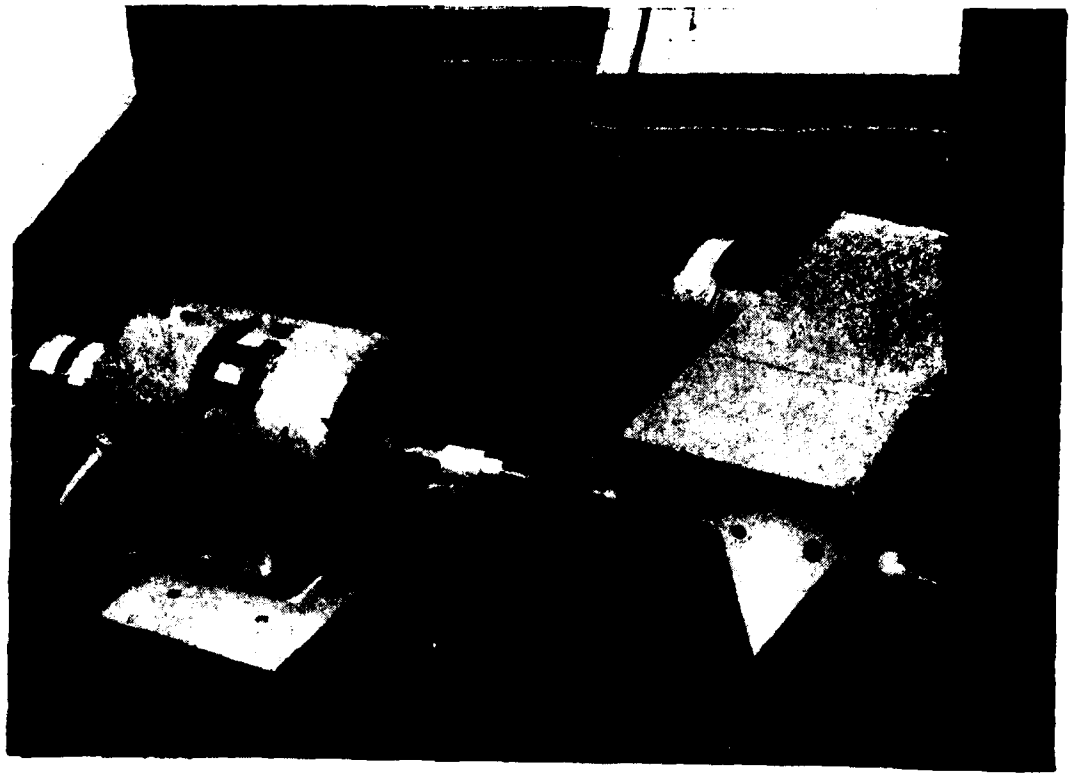

Fig. 3 Exhaust system for tunnel, showing arrangement to produce flow oscillation.

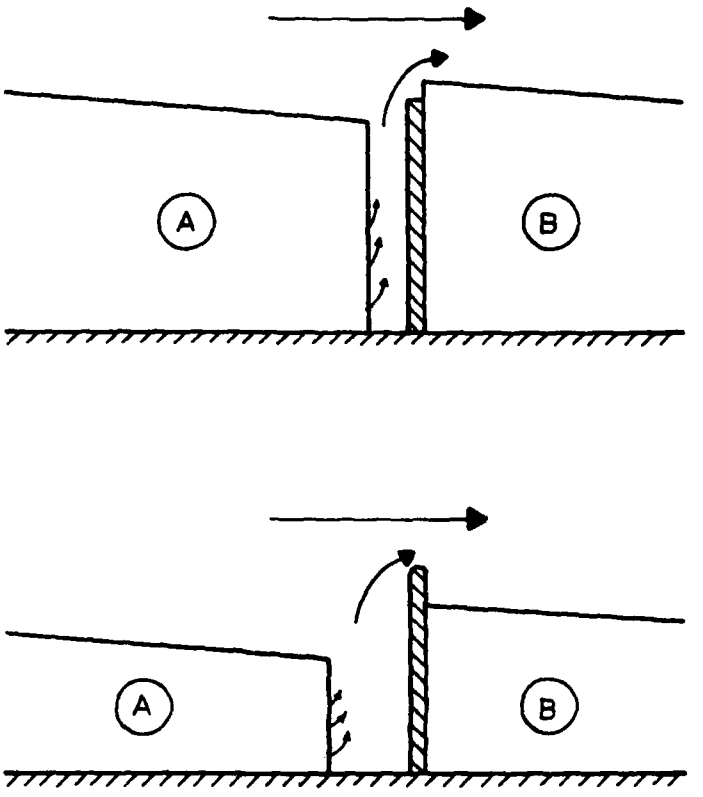

Fig. 4 Details of the flow channel in the vicinity of segment ends (shown at two different times during burning: not to scale).

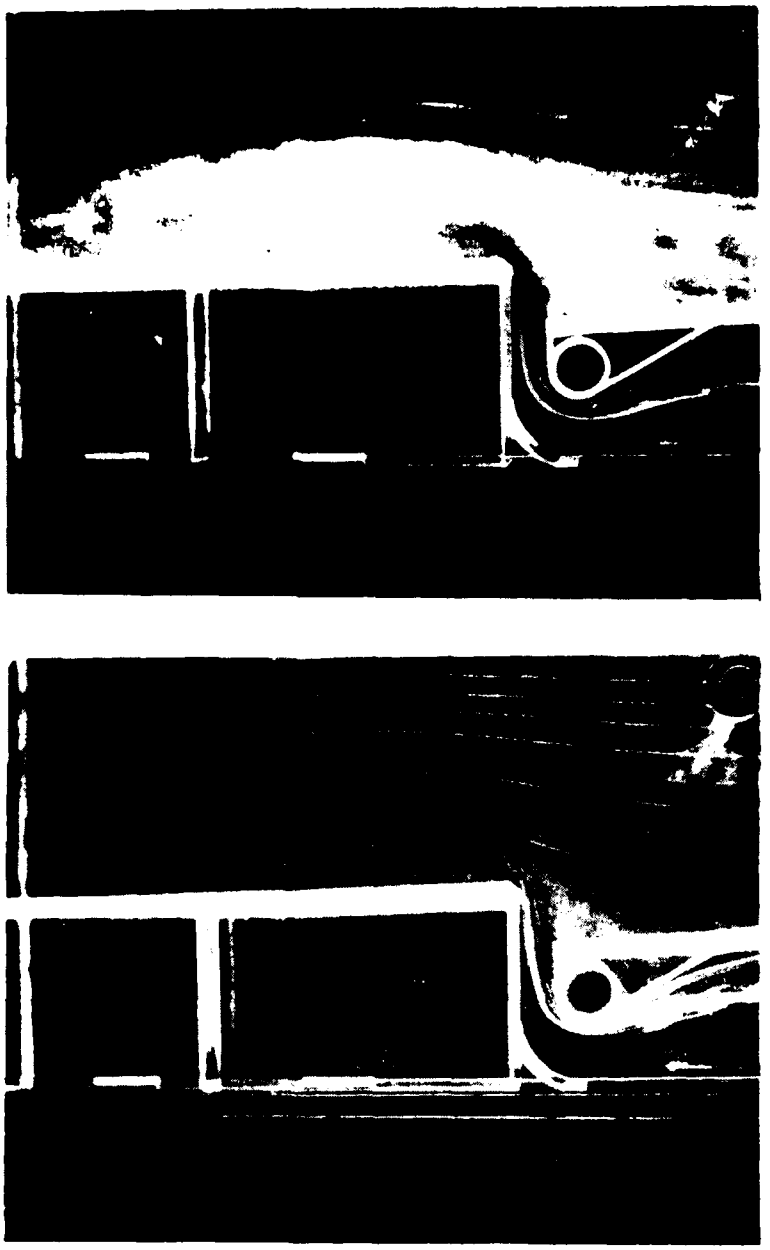

Fig. 5 Two pictures of test model in smoke tunnel, showing separated flow in step-slot region. Flow right to left.

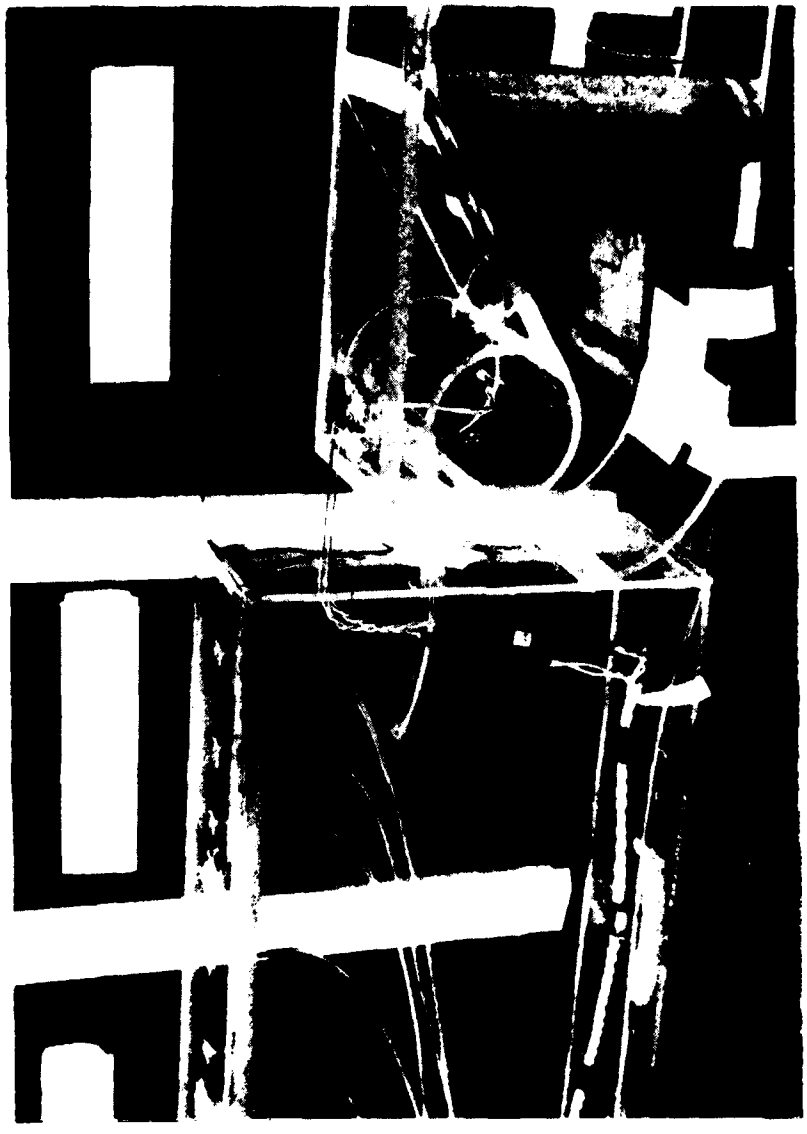

Fig. 6 Standard model configuration showing locations of hot wires and smoke inlets.
a) Photograph with tunnel wall removed

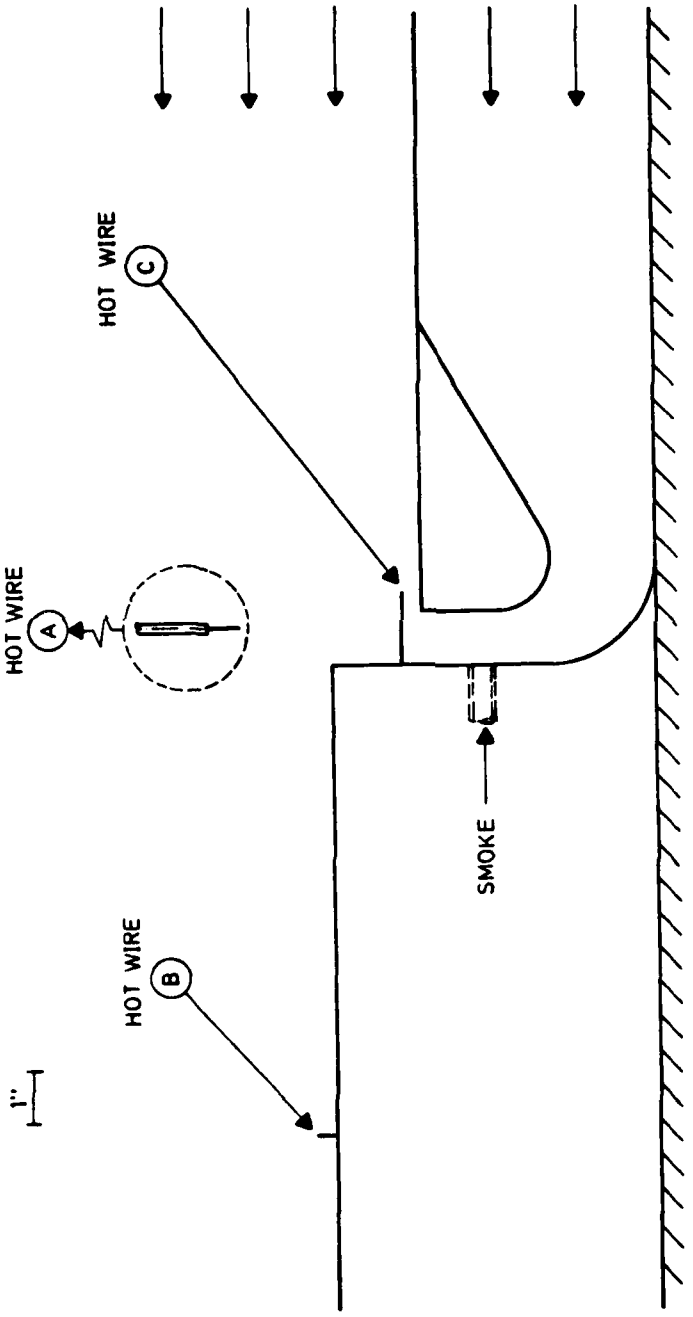

Fig. 6 Standard model configuration showing locations of hot wires and smoke inlets

b) Scale sketch

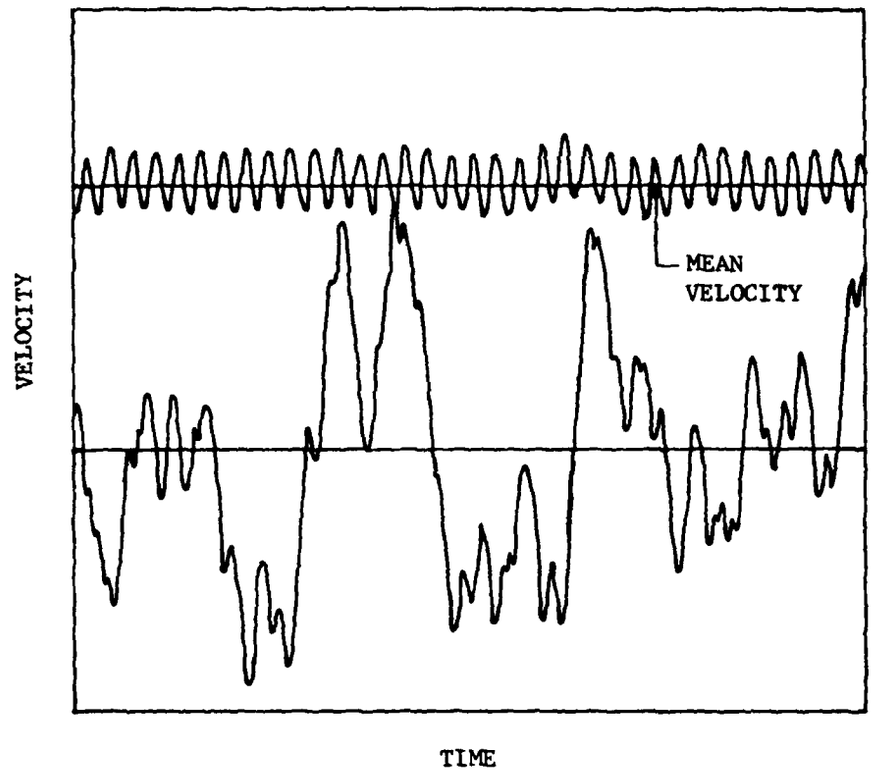

Fig. 7 Pen recorder trace of velocity fluctuations measured at positions A and B (mainstream flow velocity 10 m/sec).

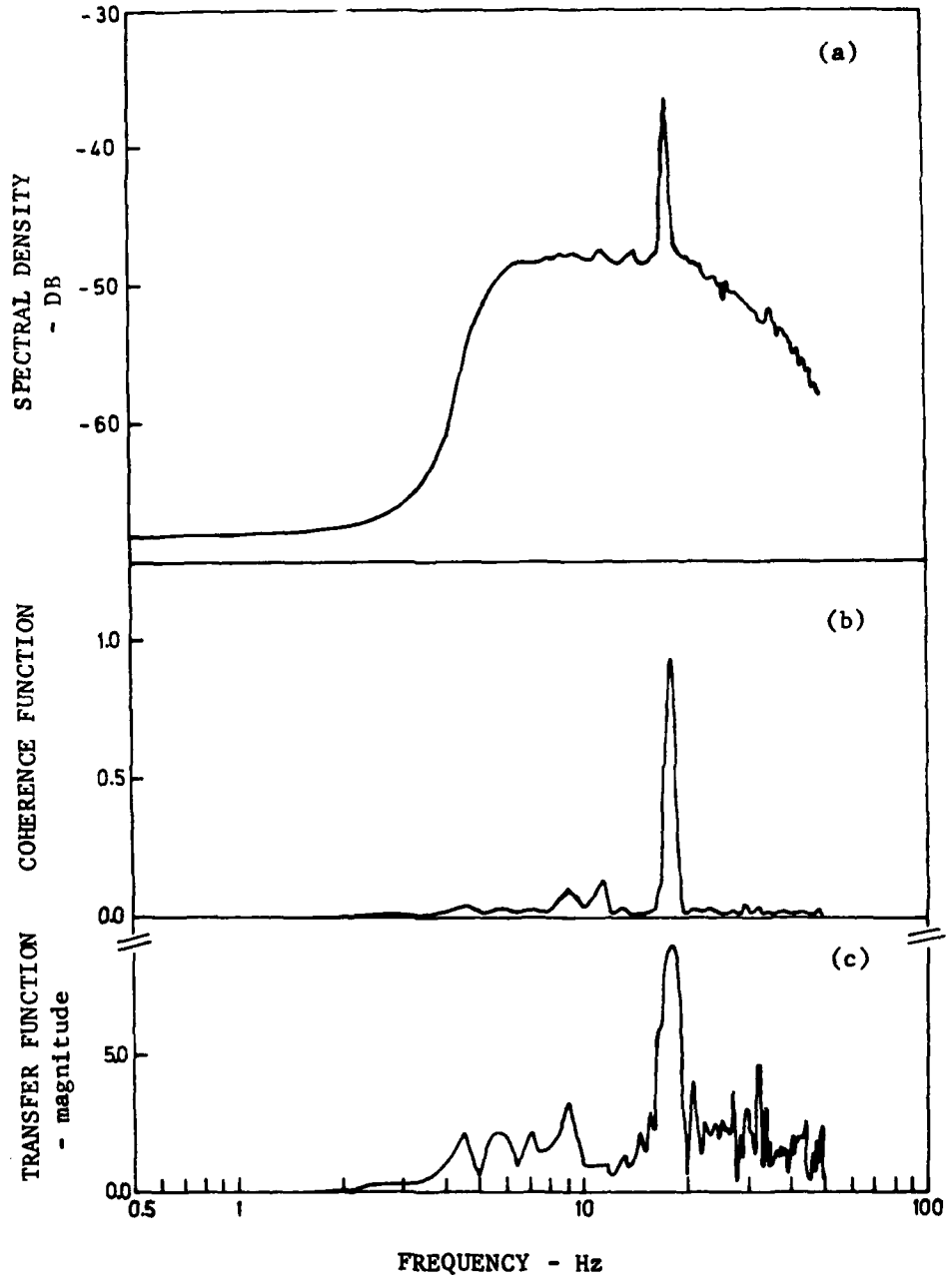

Fig. 8 Results of Fourier analysis (freestream mean velocity 10 m/sec, driven frequency 18 Hz).
a) Power spectrum of record from Position B
b) Coherence function between velocity fluctuations at A and B
c) Magnitude of transfer function between velocity fluctuations at A and B

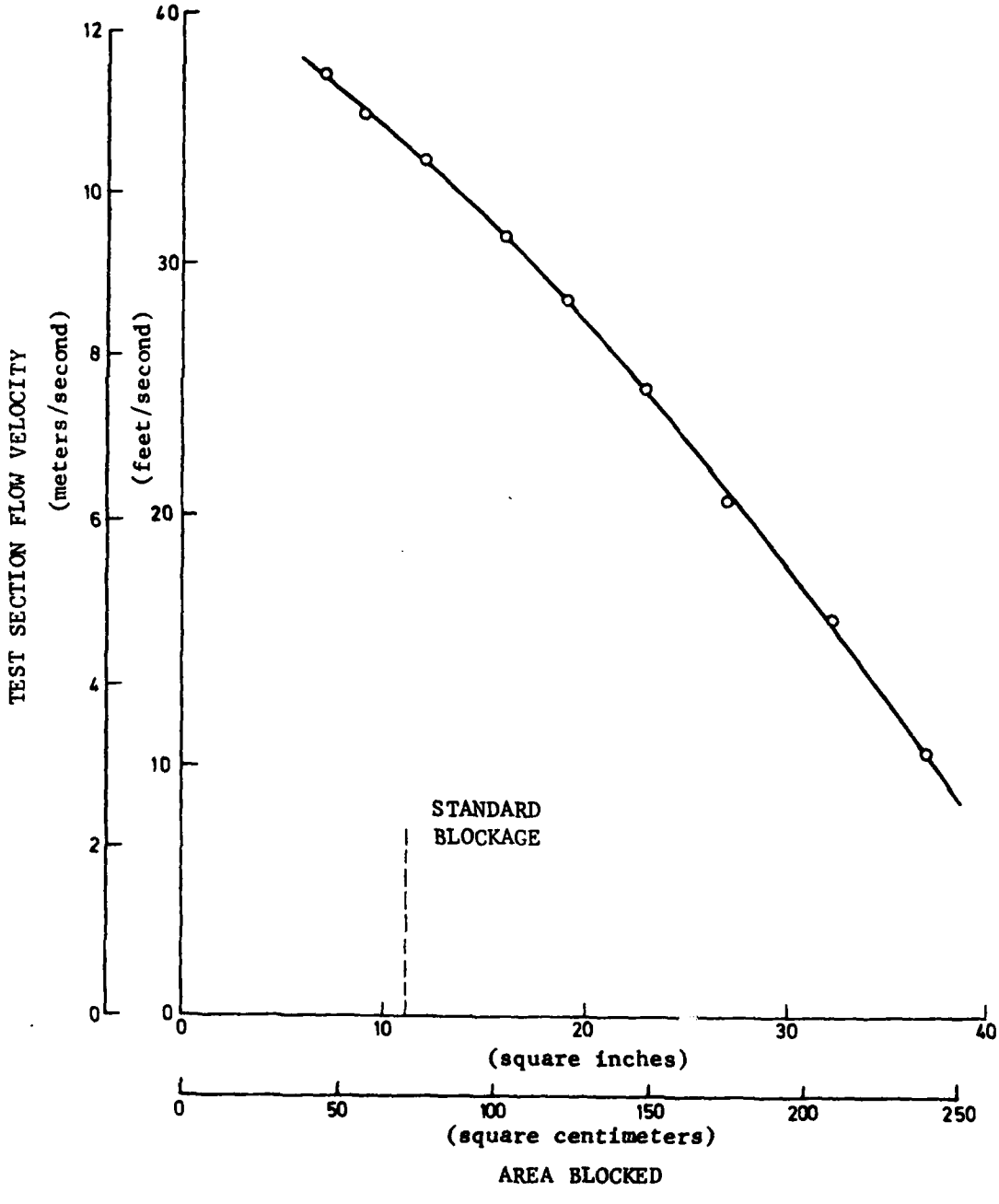

Fig. 9 Variation of tunnel freestream velocity with exhaust duct blockage.

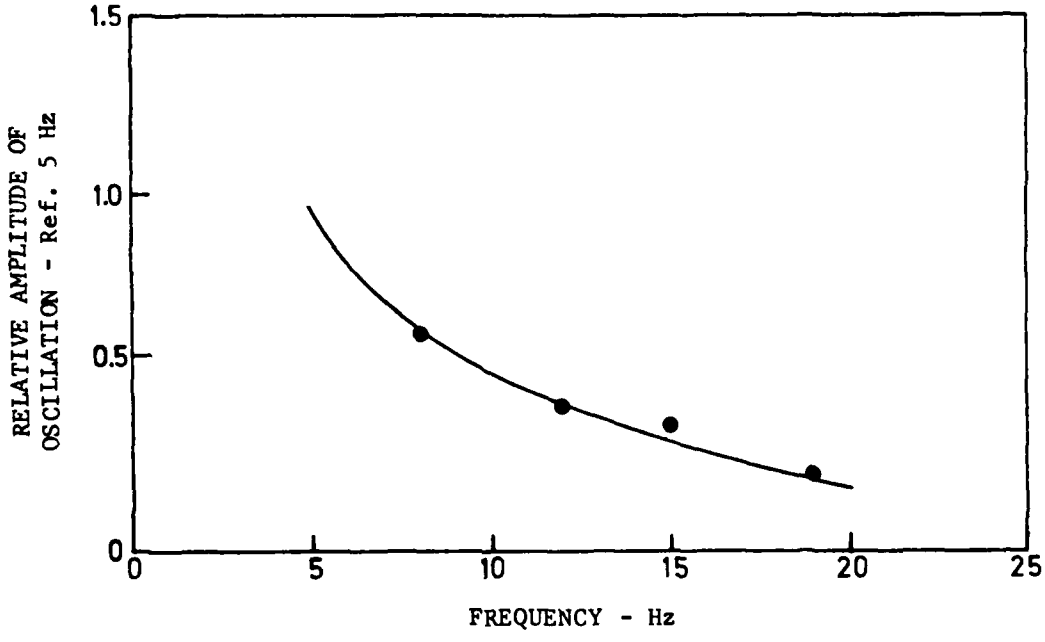

Fig. 10 Effect of frequency on amplitude of oscillation of freestream velocity.

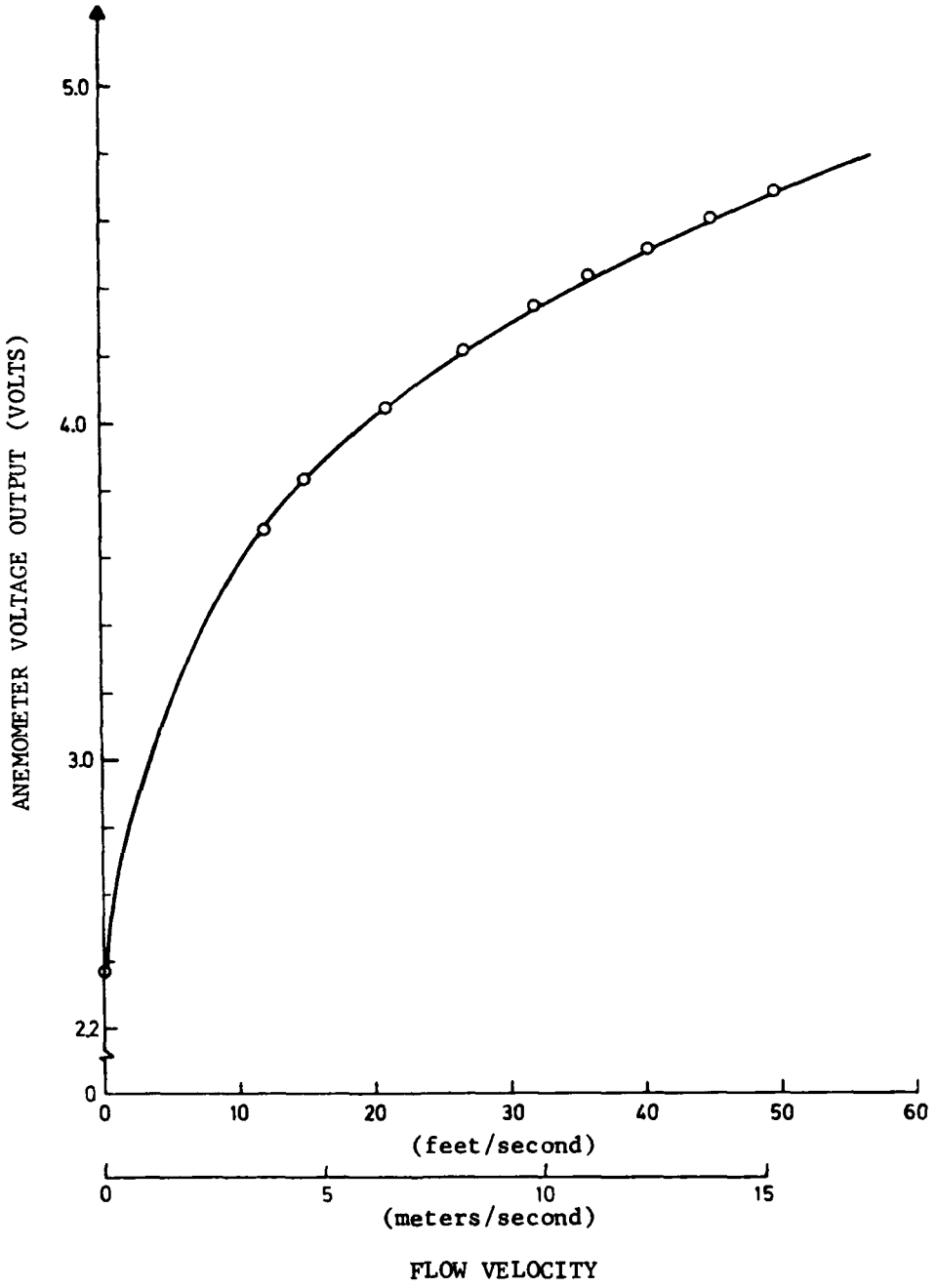

Fig. 11. Typical hot-wire calibration.

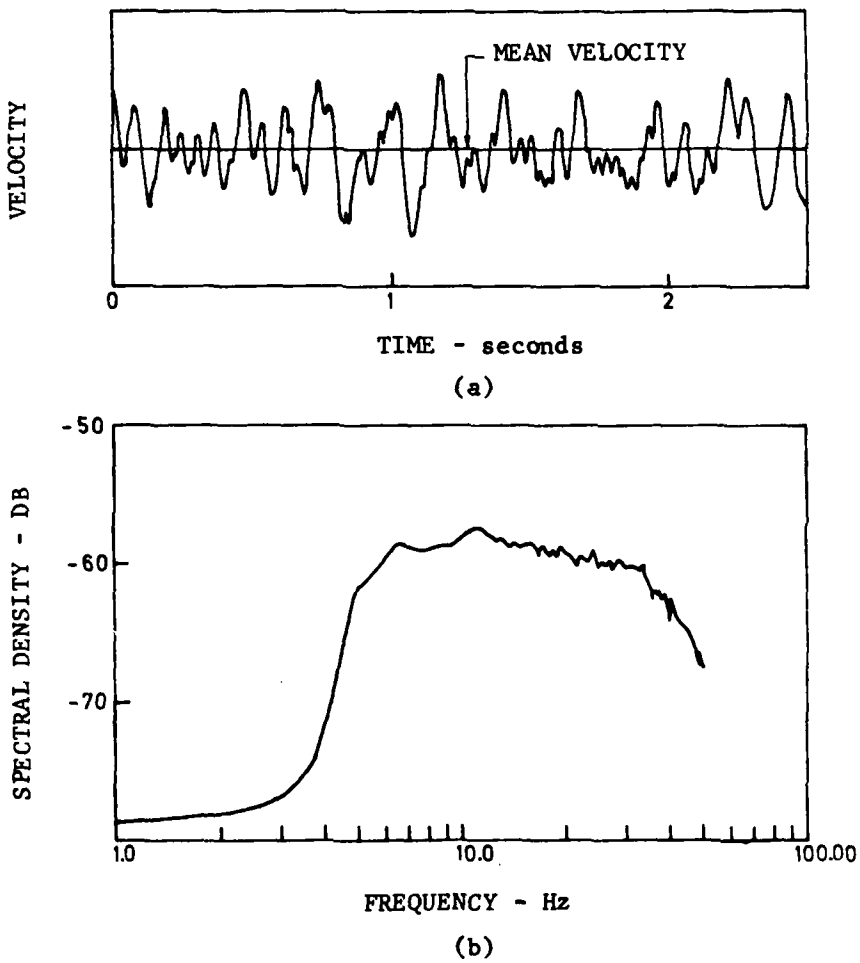

Fig. 12 Sample velocity fluctuations at position B in the absence of driven oscillations (freestream mean velocity = 10 m/sec):

a) direct recording
b) spectrum

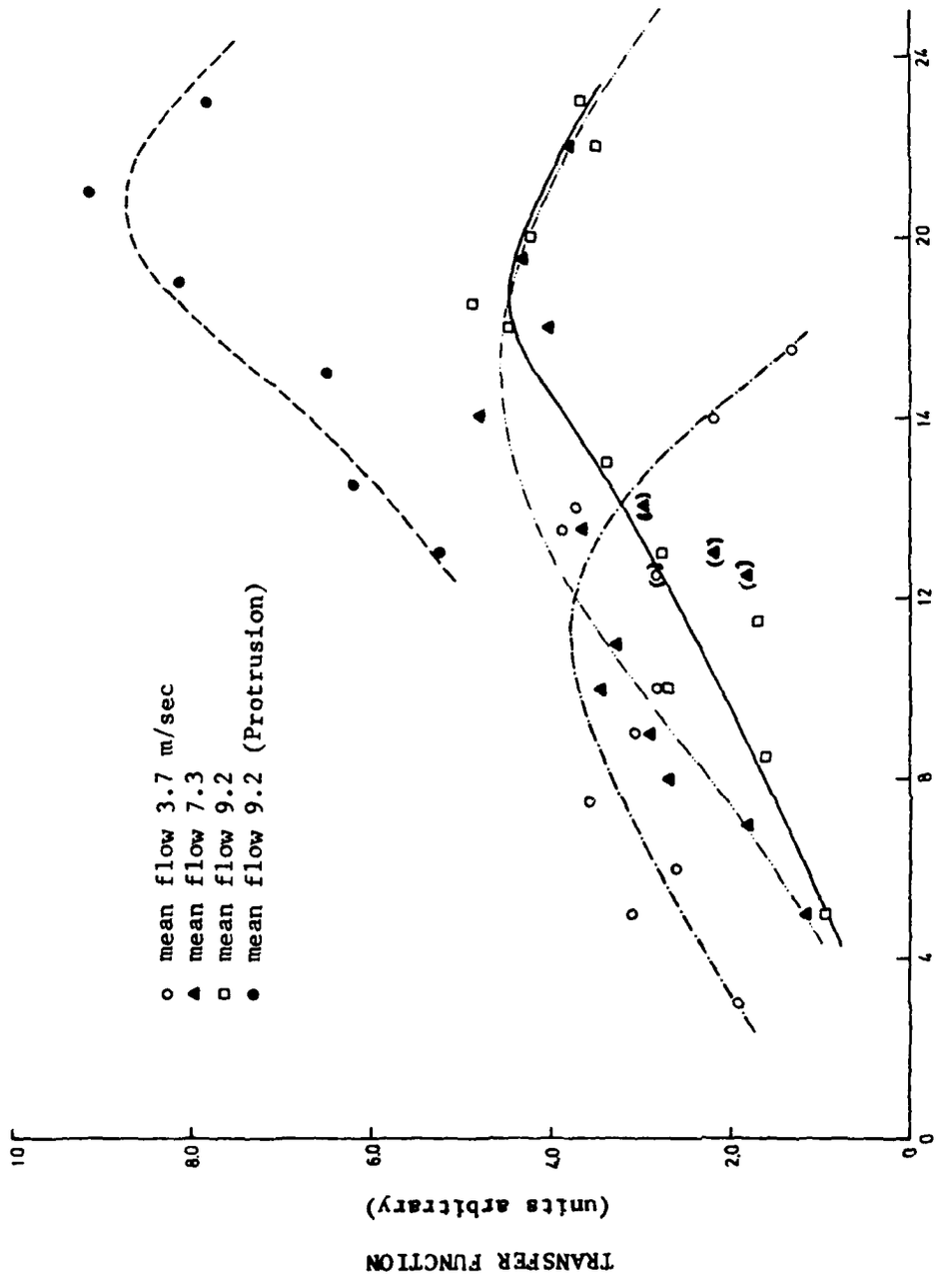

Fig. 13 Transfer function between freestream and separated flow (velocity fluctuations at driver frequency, measured at positions A and B of Fig. 6b). Data points in parenthesis correspond to low coherence between A and B, and were ignored in curve fitting.

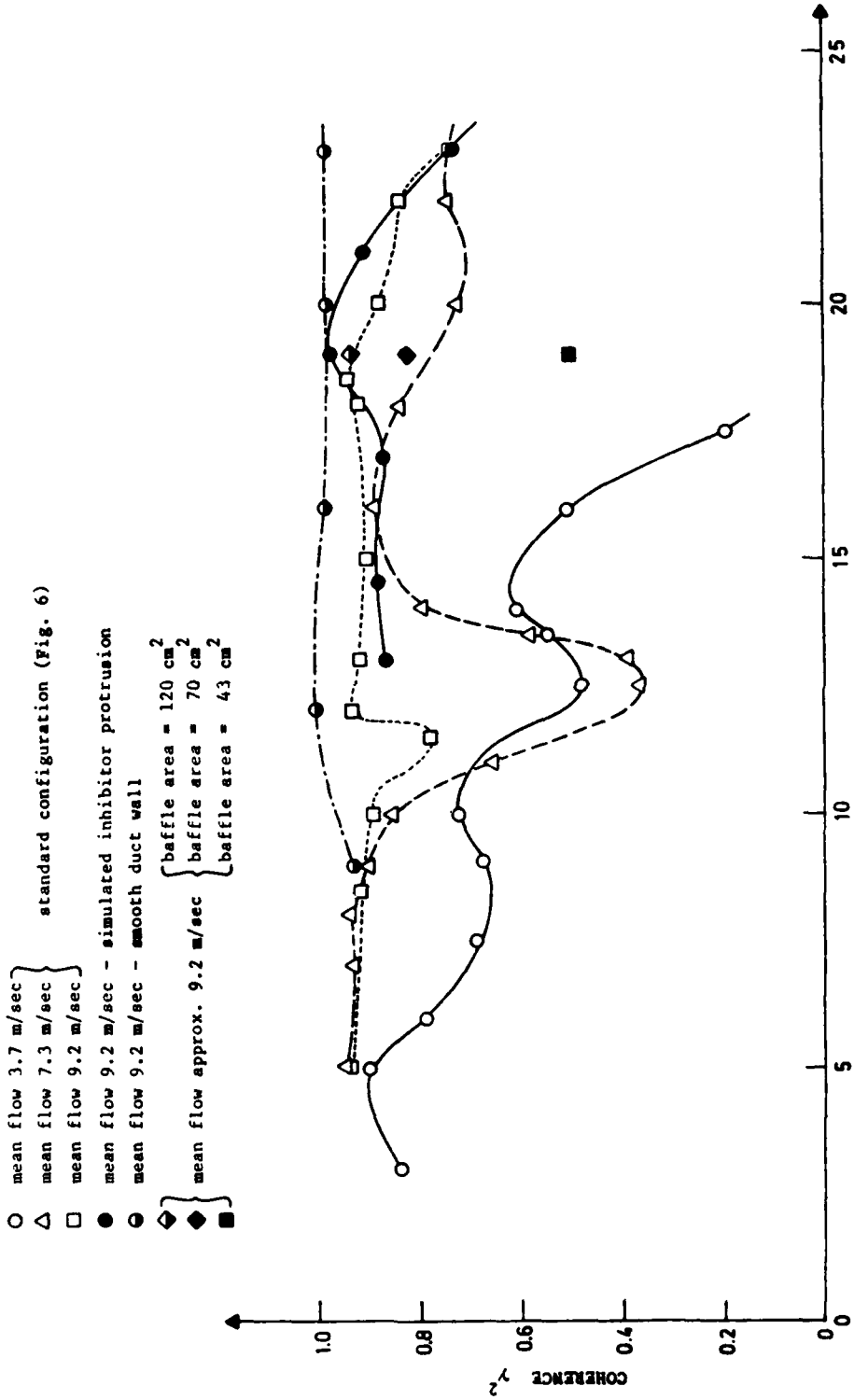

Fig. 14 Driven-frequency coherence between freestream and separated flow (velocity fluctuations, measured at Positions A and B, Fig. 6b).

INITIAL DISTRIBUTION

1 Assistant Deputy Chief of Naval Material for Laboratory Management
8 Naval Air Systems Command
- AIR-00D4 (2)
- AIR-3021 (2)
- AIR-330 (1)
- AIR-330B, Robert Brown (1)
- AIR-330D (1)
- AIR-536 (1)

4 Chief of Naval Operations
2 Chief of Naval Material
- MAT-07 (1)
- MAT-08 (1)

6 Naval Sea Systems Command
- SEA-003 (1)
- SEA-62R2
  - Cassel (1)
  - Murrin (1)
- SEA-9961 (1)
- SEA-99612 (2)

7 Chief of Naval Research, Arlington
- ONR-100 (1)
- ONR-102 (1)
- ONR-400 (1)
- ONR-420 (1)
- ONR-472 (1)
- ONR-473
  - Richard Miller (1)
  - James R. Patton, Jr. (1)

2 Naval Ordnance Station, Indian Head
- Code 525, Peter Stang (1)
- Technical Library (1)

3 Naval Postgraduate School, Monterey
- Code 57, Fuhs (1)
- Code 57NT, Netzer (1)
- Technical Library (1)

3 Naval Research Laboratory
- Code 2021 (1)
- Code 6130, Chemistry Division (1)
- Technical Library (1)

2 Naval Surface Weapons Center Detachment, White Oak Laboratory, Silver Spring
- Code 240, Sigmund Jacobs (1)
- G. B. Wilmot (1)

1 Naval Underwater Systems Center, Newport (Code 5B331, Robert S. Lazar)
1 Naval Weapons Evaluation Facility, Kirtland Air Force Base (Code 401)
2 Navy Strategic Systems Project Office
SP-2731, Roy Kinert (1)
NSP-2731, Throckmorton (1)
3 Army Armament Research and Development Command, Dover
DRDAR-LCA-G, C. Lenchitz (1)
DRDAR-LCE, J. Picard (1)
DRDAR-SCA-PE, L. Stiefel (1)
1 Army Missile Command, Redstone Scientific Information Center, Redstone Arsenal (DRSMI-R, Dr. R. G. Rhoades)
3 Army Ballistic Research Laboratories, Aberdeen Proving Ground
DRDAR-BLP
Austin W. Barrows (1)
Ingo W. May (1)
DRDAR-TSB-S (STINFO) (1)
1 Rock Island Arsenal (Edward Haug)
1 Air Force Armament Laboratory, Eglin Air Force Base (DLDL, Otto K. Heiney)
1 Air Force Rocket Propulsion Laboratory, Edwards Air Force Base (AFRPL/CA, Dr. R. Weiss)
1 Air Force Rocket Propulsion Laboratory, Edwards Air Force Base (AFRPL/MKP, Robert Geisler)
1 Air Force Rocket Propulsion Laboratory, Edwards Air Force Base (AFRPL/PAC, Wilbur C. Andrepont)
2 Air Force Office of Scientific Research
Leonard Caveny (1)
Bernard T. Wolfson (1)
12 Defense Technical Information Center
1 National Aeronautics & Space Administration (Code RP, Frank W. Stephenson, Jr.)
2 George C. Marshall Space Flight Center
SE-ASTN-PEA, John Q. Miller (1)
Richard J. Richmond (1)
1 Lewis Research Center (Richard J. Priem)
1 Lyndon B. Johnson Space Center (EP, Joseph G. Thibodaux)
1 Aerojet Solid Propulsion Company, Sacramento, CA (Dept 4350, M. Ditore) via AFPRO
1 Aeronautical Research Associates of Princeton, Inc., Princeton, NJ (R. A. Beddini)
1 Aerospace Corporation, Los Angeles, CA (Ellis M. Landsbaum)
1 Allegany Ballistics Laboratory, Cumberland, MD (Roy R. Miller)
1 Atlantic Research Corporation, Alexandria, VA (Merrill K. King)
1 Battelle Memorial Institute, Columbus, OH (Abbott A. Putnam)
1 Brigham Young University, Provo, UT (673/W1dB, M. Beckstead)

1 California State University Sacramento, Sacramento, CA
(School of Engineering, Frederick H. Reardon)
1 Calspan Corporation, Buffalo, NY (Edward B. Fisher)
3 Georgia Institute of Technology, Atlanta, GA
Ben T. Zinn (1)
Edward W. Price (1)
Warren C. Strahle (1)
1 General Applied Science Laboratory, Westbury Long Island, NY
(John Erdos)
1 General Dynamics Corporation, Pomona Division, Pomona, CA
(Paul L. Boettcher)
2 Hercules Incorporated, Bacchus Works, Magna, UT
Ken McCarty (1)
Ronald L. Simmons (1)
1 Hercules, Incorporated, McGregor, TX (William G. Haymes)
1 Institute for Defense Analyses, Arlington, VA (R. C. Oliver)
2 Jet Propulsion Laboratory, Pasadena, CA
Fred E. C. Culick (1)
Leon D. Strand (1)
1 John Hopkins University, Applied Physics Laboratory, Laurel, MD
(Chemical Propulsion Information Agency, Thomas W. Christian)
2 Lockheed Missiles and Space Company, Sunnyvale, CA
J. Linsk (1)
3 Lockheed Palo Alto Research Laboratory
R. Byrd (1)
G. Lo (1)
H. Marshall (1)
1 Pennsylvania State University, State College, PA
(Applied Research Lab., Gerard M. Faeth)
1 Princeton Combustion Research Laboratories, Princeton, NJ
(M. Summerfield)
1 Purdue University, West Lafayette, IN (School of Mechanical
Engineering, John R. Osborn)
1 Rockwell International Corporation, Canoga Park, CA
(BA08, Joseph E. Flanagan)
1 Science Applications, Inc., Woodland Hills, CA (R. B. Edelman/Suite 423)
1 Southwest Research Institute, San Antonio, TX
(Fire Research Section, William H. McLain)
1 TRW Systems, Inc., Redondo Beach, CA (A. C. Ellings)
1 Thiokol Corporation, Huntsville Division, Huntsville, AL
(David A. Flanigan)
1 Thiokol Corporation, Wasatch Division, Brigham City, UT
1 United Technologies Corporation, East Hartford, CT (R. H. W. Waesche)
1 United Technologies Corporation, Sunnyvale, CA
(Chemical Systems Division, Robert S. Brown)
1 Universal Propulsion Company, Inc., Phoenix, AZ

1 University of California, San Diego, La Jolla, CA
(AMES Dept, Forman A. Williams)
1 University of Illinois, Urbana, IL (AAE Dept., Herman Krier)
1 University of Southern California, Los Angeles, CA
(Mechanical Engineering Dept/OHE200, M. Gerstein)
2 University of Utah, Salt Lake City, UT
Dept of Chemical Engineering, Alva D. Baer (1)
G. A. Flandro (1)
2 Whittaker Corporation, Bermite Division, Saugus, CA
L. Bloom (1)
L. LoFiego (1)
1 University of Waterloo, Ontario, Canada (Department of Mechanical Engineering, Clarke E. Hermance) via Naval Air Systems Command (AIR-960)

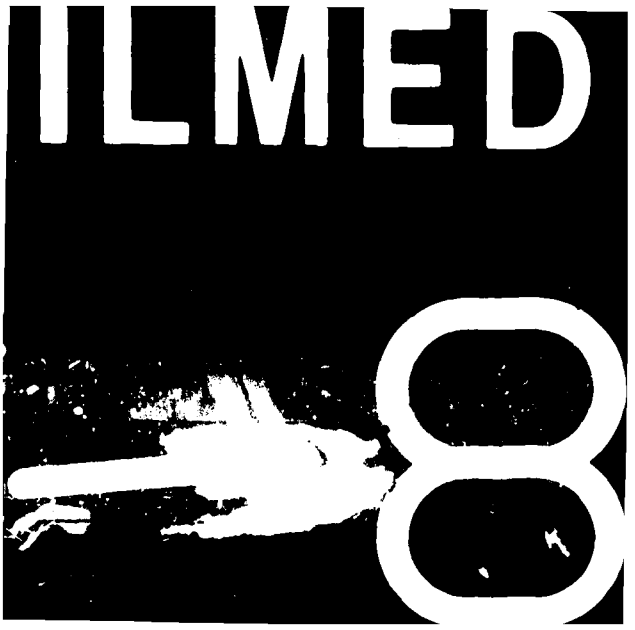
ILMED
8